Single isomer of indene-C_{70} bisadduct – isolation and performance in bulk heterojunction solar cells

Wallace W. H. Wong,* Jegadesan Subbiah, Jonathan M. White, Helga Seyler, Bolong Zhang, David J. Jones, Andrew B. Holmes.

School of Chemistry, Bio21 Institute, University of Melbourne, 30 Flemington Road, Victoria, 3010, Australia.

KEYWORDS: Fullerene bisadduct, regioisomer, chromatographic isolation, organic solar cells

ABSTRACT: Indene-C_{70} bisadduct ($IC_{70}BA$) is a high performance electron acceptor material consisting of a mixture of regioisomers. A single isomer of the $IC_{70}BA$ was isolated by careful chromatographic separation. The structure of this isomer was confirmed by various analytical techniques including single crystal X-ray analysis. The isomer showed superior performance to other isomer mixtures of $IC_{70}BA$ in bulk heterojunction solar cells using poly(3-hexylthiophene) as the donor material.

The electron deficient character and semiconducting properties of fullerenes have made them ideal acceptor materials in bulk heterojunction (BHJ) organic solar cells (OSC).[1] Several classes of fullerene derivatives have emerged as efficient electron acceptors in OSC devices.[1] One of the most successful derivatives is the Diels-Alder bisadduct of indene and fullerene, ICBA (Figure 1a).[2,3] The benchmark BHJ device with poly(3-hexylthiophene) (P3HT) as donor material is currently 7.5% for the C_{60} derivative ($IC_{60}BA$)[4] and 7.4% for the C_{70} derivative ($IC_{70}BA$).[5] The feature of bisadducts that enables improved device performance is their elevated lowest unoccupied molecular orbital (LUMO) energy level compared with monoadducts.[6,7] As the open circuit voltage (V_{oc}) of a BHJ device is dependent on the LUMO energy level of the acceptor material and the energy of the highest occupied molecular orbital (HOMO) of the donor material, a higher LUMO level of the acceptor leads to a higher V_{oc}.[7]

While the ease of synthesis[8] and existence of a high LUMO level are great advantages for ICBA compounds, it is generally acknowledged that these materials demonstrate large variations in performance when used in devices with different donor materials. Expected performance improvements have been observed when comparing P3HT devices with PCBM and ICBA. However, only a few examples of other electron donor materials show a device performance improvement when comparing ICBA with PCBM.[7] The reason for this observation can depend on many factors including solubility, semiconducting properties and the morphology of the donor-acceptor blend films.

One important factor, that is often overlooked, is that ICBA compounds have always been used as mixtures of isomers in OSC devices.[9,10] Surprisingly, it is only recently that two studies have tried to address this issue but they either did not isolate single pure bisadducts[9] or the isolated derivative was not used in solar cell devices due to the small quantity of material available.[10] In this study, isolation of a single geometric isomer of C_{70} bisadduct was achieved in reasonable quantity and this material showed superior performance in devices compared with isomer mixtures.

The synthesis of C_{70} bisadducts typically leads to a mixture of three major regiosiomers; so-called 5, 2 and 12 o'clock isomers (Figure 1c). This is because the α bonds stemming from the pentagonal ends of the C_{70} molecule are the most reactive (Figure 1b).[11] Taking into account the *in*/*out* indene adduct arrangements, there should be eight major geometric isomers for $IC_{70}BA$ of which seven are chiral (Figure 1c).

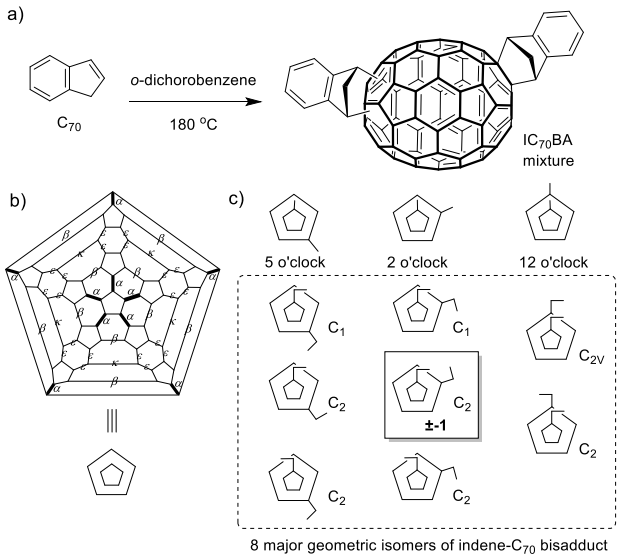

Figure 1. a) Diels-Alder addition of indene to C_{70}; b) Schlegel diagram of C_{70} and c) illustrations of C_{70} bisadducts and their symmetry groups.

In this study, the aim was to compare the performance of various $IC_{70}BA$ isomer fractions in BHJ solar cells. The $IC_{70}BA$ isomer mixture was carefully separated using conventional and high performance liquid chromatography (HPLC). One fraction was identified as a single geometric isomer that produced a crystalline sample whose structure was solved by single crystal X-ray analysis. This pure crystalline sample afforded improved efficiency for BHJ devices with P3HT compared with the use of isomeric mixtures of $IC_{70}BA$.

The mixture of $IC_{70}BA$ isomers were synthesized by adding indene portionwise to a stirred solution of C_{70} at 180 °C in *o*-dichlorobenzene under nitrogen atmosphere (Figure 1a). The reaction was closely monitored by thin layer chromatography (SiO_2, cyclohexane/toluene 9:1) to optimize the formation of

the bisadduct. After adding 10 equivalents of indene over the course of 10 hours, the product mixture was separated by flash chromatography (SiO_2, cyclohexane/toluene 9:1). The product distribution isolated was as follows: monoadduct $IC_{70}MA$ 19%, bisadducts $IC_{70}BA$ 48% and multiadducts 11%. Two fractions of $IC_{70}BA$ were obtained in a 2:1 ratio (see experimental for exact amounts).

The ^1H NMR spectrum of $IC_{70}BA$ fraction 1 from the flash column was rather complex indicating that it is a mixture of a number of isomers (Figure 2a). Interestingly, the ^1H NMR spectrum of fraction 2 is much simpler and two major sets of resonances can be identified in the aliphatic region (Figure 2b, 2 to 5 ppm). Considering the geometry of the bisadducts, it is apparent that fraction 2 contained bisadduct isomers with C_2 or C_{2v} symmetry (Figure 1c).

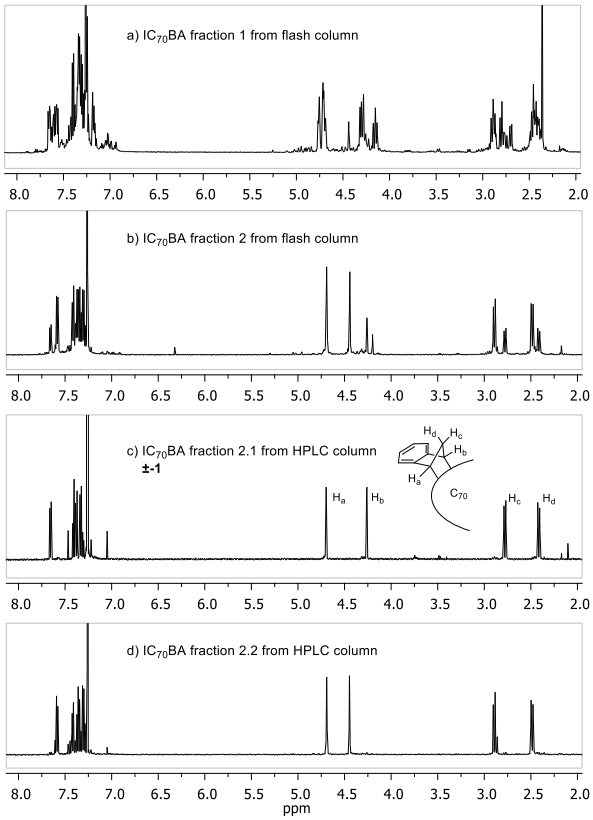

Figure 2. ^1H NMR spectrum of $IC_{70}BA$ a) fraction 1, b) fraction 2, c) fraction 2.1 and d) fraction 2.2 from HPLC separation.

Encouraged by the simplified ^1H NMR spectrum of fraction 2, HPLC separation was performed on a Cosmosil® Buckyprep-D column (4.6 ID × 250 mm, toluene, 1 mL/min, UV detection 325 nm). The chromatograms of various $IC_{70}BA$ fractions are shown in Figure 3. One major geometric isomer was observed in fraction 2.1 and there appeared to be two isomers in fraction 2.2. While assignments was made for the clear sets of resonances in the ^1H NMR spectrum of fractions 2.1 and 2.2, it was still not possible to unequivocally determine the identity of the isomers (Figure 2c and d). The ^{13}C NMR data of fraction 2.2 suggested that the major isomer in this fraction has high C_{2v} symmetry and this is most likely to be the 12 o'clock isomer (Figure S9 and 1c). UV-vis spectra of fraction 2.1 and 2.2 were recorded to provide further data for isomer identification (Figure 4). It is well-known that different regioisomers of fullerene bisadducts show distinctive UV-vis absorption profiles.[12,13] Keeping in mind the electronic influence of the substituent on the fullerene molecule, the spectral comparison of the $IC_{70}BA$ isomer fractions with C_{70} bismalonate derivatives[12] suggested that fraction 2.1 and 2.2 were likely to be the 2 and 12 o'clock regioisomers respectively (Figure 4). This is in agreement with the interpretation of the ^{13}C NMR data for fraction 2.2.

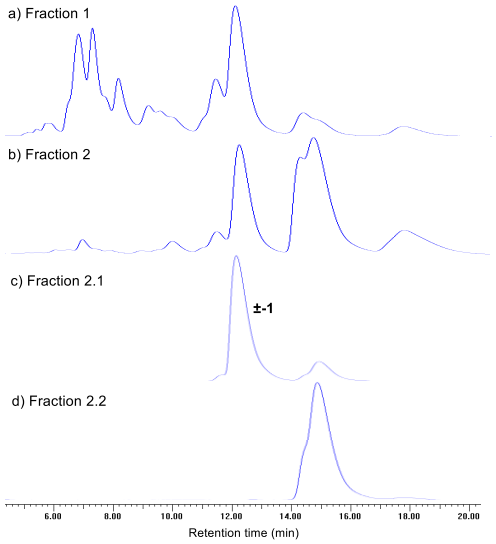

Figure 3. HPLC chromatograms of $IC_{70}BA$ a) fraction 1, b) fraction 2, c) fraction 2.1 and d) fraction 2.2 using a Cosmosil® Buckyprep-D column.

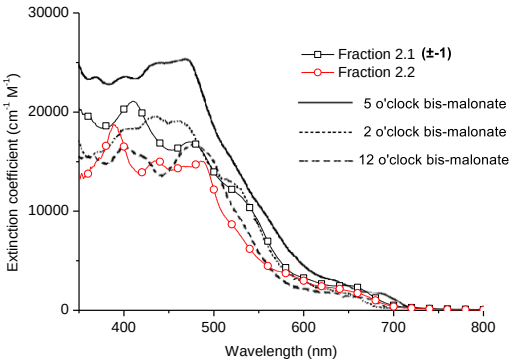

Figure 4. UV-vis spectrum of $IC_{70}BA$ fractions 2.1 and 2.2 in chloroform solution and the spectrum of C_{70} bis-malonate isomers were taken from the literature for comparison.[12]

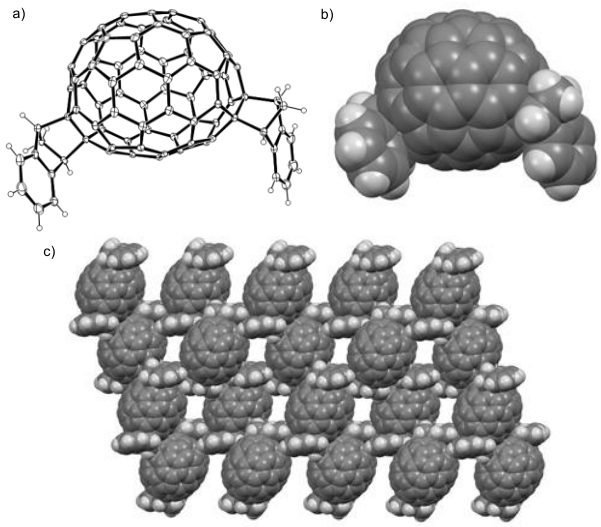

Figure 5. Structure obtained by X-ray analysis of **±-1** crystals grown from chloroform solution of fraction 2.1 (see Figure 3) a) thermal ellipsoid illustration; b) space filling model and c) packing diagram where disordered $CHCl_3$ solvent molecules have been omitted for clarity.

Fractions 2.1 and 2.2 were further purified by recrystallization from chloroform. Crystals obtained from 2.1 were examined using X-ray crystallography and the structure of the isomer for fraction 2.1 was unequivocally revealed as one of the 2 o'clock isomers, (±)-*in,in*-1',1",4',4"-tetrahydrobis[1,4]methanonaphtho[2',3':8,25;2",3":33,34]-(C70-D5h)[5,6]fullerene **±-1** (Figure 5 and 1c). The crystal packing diagram shows the arrangement of alternating rows of enantiomeric pairs with chloroform filling small voids between the fullerenes (Figure 5c). The nearest inter-fullerene distance is 3.21 Å.

To complete the characterization, thermal and electrochemical properties of all the isomeric fractions were investigated. $IC_{70}BA$ isomers from fractions 1 and 2 decomposed at 250 °C probably resulting from a retro Diels-Alder process (see Supporting Information). The electrochemical properties of the isomeric fractions were essentially the same with the first reduction potential occurring at -1.3 V verses ferrocene/ferrocenium (see Supporting Information). The LUMO energy level of the $IC_{70}BA$ fractions is therefore -3.5 eV which is consistent with previous literature reports.[7,10]

The $IC_{70}BA$ isomer fractions as well as the overall isomer mixture were used in BHJ OSC devices to compare their performance. A device architecture of ITO/PEDOT:PSS/active layer/Ca/Al was used with the ratio of donor material, P3HT, and $IC_{70}BA$ isomers set at 1:1 by weight and *o*-dichlorobenzene was used as processing solvent (Figure 6a). Table 1 summarizes the device performance of the various solar cells and the following characteristic parameters are given: short-circuit current density (J_{sc}), open-circuit voltage (V_{oc}), fill factor (*FF*), and power-conversion efficiency (PCE). A significant increase in PCE of the devices were observed when the pure bisadduct **±-1** from fraction 2.1 was used compared to other isomeric mixtures. An average PCE of 5.9% was recorded for devices containing **±-1** (10 cells) and this value is higher than P3HT/$IC_{70}BA$ devices reported in the literature without the use of solvent annealing or additives.[5] The increased device performance stemmed from higher current density and fill factor (Figure 6b and Table 1).

Table 1 Photovoltaic performance of BHJ devices using P3HT and various $IC_{70}BA$ fractions in the active layer. The data shown are the average values obtained from 10 devices with standard deviation.

$IC_{70}BA$ fractions	V_{oc} (V)	J_{sc} (mA/cm^2)	*FF* (%)	PCE (%)
mixture	0.82 ±0.01	9.3 ±0.3	62 ±3	4.7 ±0.35
1	0.80 ±0.01	8.5 ±0.2	56 ±3	3.9 ±0.20
2	0.84 ±0.01	9.7 ±0.4	65 ±3	5.3 ±0.40
±-1 (2.1)	0.86 ±0.01	10.3 ±0.2	67 ±2	5.9 ±0.25
2.2	0.84 ±0.02	9.5 ±0.2	60 ±4	4.8 ±0.30

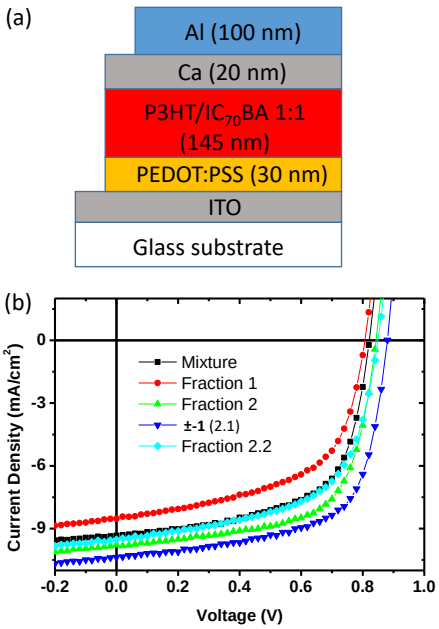

Figure 6. (a) Schematic diagram of BHJ device configuration and (b) J-V curves of the BHJ solar cells based on P3HT and various $IC_{70}BA$ fractions.

To examine the photocurrent contribution of the active layers, the optical absorption spectra and external quantum efficiency (EQE) curves for the BHJ devices were recorded (Figure 7). It is interesting to note that the optical absorption of the devices containing the $IC_{70}BA$ mixture and fractions 1 and 2 showed higher absorbance at 500 nm but this was not reflected in their EQE spectra. On the other hand, the best performing device containing **±-1** showed significant photocurrent enhancement at 410 nm (Figure 7b). In fact, the maximum EQE of 70% at 410 nm is higher than the EQE of the best P3HT/$IC_{70}BA$ device in the literature which employed solvent annealing and additives to boost performance.[5] This photocurrent contribution can be assigned to the $IC_{70}BA$ material. This means more photocurrent was generated from the acceptor when using isomer **±-1** despite lower absorbance in that spectral region of the device compared to other $IC_{70}BA$ fractions. This

observation may be attributed to better charge transport properties of the crystalline **±-1** isomer and superior donor-acceptor film morphology.

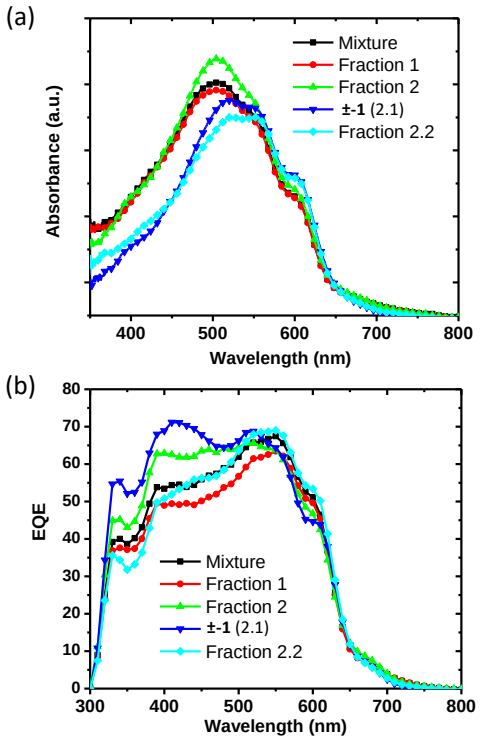

Figure 7. (a) UV-vis absorption spectrum and (b) external quantum efficiency (EQE) curves of the BHJ solar cells based on P3HT and various $IC_{70}BA$ fractions. Note that the UV-vis spectra were recorded for the devices with the absorbance of the ITO/PEDOT:PSS layers subtracted.

The charge transport properties of $IC_{70}BA$ isomers were examined using space charge limited current (SCLC) measurements (see Supporting Information for experimental details). The electron mobility for fractions 2, 2.1 (**±-1**) and 2.2 were calculated to be 4.3, 2.1 and 0.8 × 10^{-4} cm^2/Vs respectively. These values were in an appropriate charge mobility range that would allow efficient solar cell devices with significant photocurrent contribution from the fullerene acceptor material (Figure 7b). Atomic force microscopy (AFM) was used to probe the surface morphology of the active layer films. Phase separation and similar donor-acceptor domain size was observed for films containing various $IC_{70}BA$ fractions (Figure S17). All above device characterization data showed that the single geometric isomer **±-1** (fraction 2.1) outperformed mixtures of $IC_{70}BA$ isomers primarily as a result of its purity and crystallinity.

A single geometric isomer of $IC_{70}BA$ was isolated for the first time. The promising improvements in performance of devices containing **±-1** suggested that crystallinity of the material played an important role in the device operation. This is in agreement with two recent studies where the reduction in the number of fullerene bisadduct isomers led to superior performance in devices.[9,10] While significant quantity of material was isolated through careful chromatographic separation in this study, methods to target pure regioisomers of fullerene bisadducts through controlled synthesis[13,14] are currently under investigation.

ASSOCIATED CONTENT

Supporting Information

Supporting information contains detailed experimental procedures and characterization data. This material is available free of charge via the Internet at http://pubs.acs.org.

AUTHOR INFORMATION

Corresponding Author

* wwhwong@unimelb.edu.au

ACKNOWLEDGMENT

This work was made possible by support of the Victorian Organic Solar Cell Consortium, with funding provided by the Victorian State Government Department of State Development, Business and Innovation (Energy Technology Innovation Strategy and Victorian Science Agenda) and the Australian Renewable Energy Agency (ARENA Project 2-A018). Dr W. W. H. Wong is supported by an ARENA Research Fellowship. We thank Dr Carlo Thilgen (ETH Zürich) for his advice on the choice of HPLC columns for fullerene separation and fullerene nomenclature.

REFERENCES

(1) He, Y.; Li, Y. *Phys. Chem. Chem. Phys.* **2011**, *13*, 1970.
(2) He, Y.; Chen, H.-Y.; Hou, J.; Li, Y. *J. Am. Chem. Soc.* **2010**, *132*, 1377.
(3) He, Y.; Zhao, G.; Peng, B.; Li, Y. *Adv. Funct. Mater.* **2010**, *20*, 3383.
(4) Liao, S.-H.; Li, Y.-L.; Jen, T.-H.; Cheng, Y.-S.; Chen, S.-A. *J. Am. Chem. Soc.* **2012**, *134*, 14271.
(5) Guo, X.; Cui, C.; Zhang, M.; Huo, L.; Huang, Y.; Hou, J.; Li, Y. *Energy Environ. Sci.* **2012**, *5*, 7943.
(6) Lenes, M.; Wetzelaer, G.-J. A. H.; Kooistra, F. B.; Veenstra, S. C.; Hummelen, J. C.; Blom, P. W. M. *Adv. Mater.* **2008**, *20*, 2116.
(7) Li, Y. *Chem. Asian J.* **2013**, *8*, 2316.
(8) Seyler, H.; Wong, W. W. H.; Jones, D. J.; Holmes, A. B. *J. Org. Chem.* **2011**, *76*, 3551.
(9) Meng, X.; Zhao, G.; Xu, Q.; Tan, Z. a.; Zhang, Z.; Jiang, L.; Shu, C.; Wang, C.; Li, Y. *Adv. Funct. Mater.* **2014**, *24*, 158.
(10) Matsuo, Y.; Kawai, J.; Inada, H.; Nakagawa, T.; Ota, H.; Otsubo, S.; Nakamura, E. *Adv. Mater.* **2013**, *25*, 6266.
(11) Herrmann, A.; Rüttimann, M.; Thilgen, C.; Diederich, F. *Helv. Chim. Acta* **1995**, *78*, 1673.
(12) van Eis, M. J.; Seiler, P.; Muslinkina, L. A.; Badertscher, M.; Pretsch, E.; Diederich, F.; Alvarado, R. J.; Echegoyen, L.; Pérez Núñez, I. *Helv. Chim. Acta* **2002**, *85*, 2009.
(13) Wong, W. W. H.; Diederich, F. *Chem. Eur. J.* **2006**, *12*, 3463.
(14) Sergeyev, S.; Diederich, F. *Angew. Chem. Int. Ed.* **2004**, *43*, 1738.

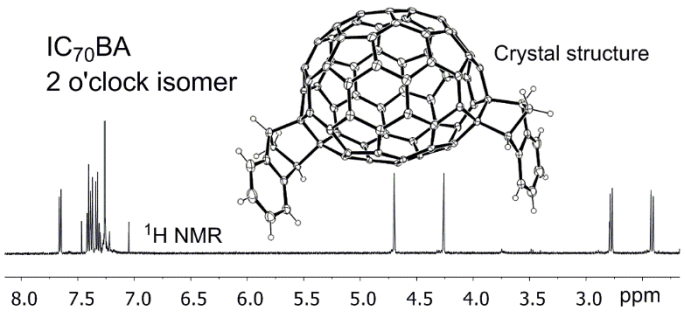
IC70BA
2 o'clock isomer
Crystal structure
1H NMR
8.0
7.5
7.0
6.5
6.0
5.5
5.0
4.5
4.0
3.5
3.0
ppm